PERGAMON

International Journal of Heat and Mass Transfer 42 (1999) 3131–3136

International Journal of HEAT and MASS TRANSFER

Heat transfer in a Bénard–Kármán vortex street in air and in water

J.C. Lecordier*, F. Dumouchel, P. Paranthoën

UMR 6614 CNRS Université de Rouen, 76821, Mont Saint Aignan Cedex, France

Received 24 July 1998; received in revised form 6 November 1998

Abstract

The near temperature field downstream of a heated ribbon is investigated experimentally in air and in water in the forced convection regime corresponding to the 2-D periodic wake. Previous measurements have shown that in a such situation the structure of the velocity fields is found similar in the two fluids when the experiments are performed at the same effective Reynolds number. When this condition is satisfied it appears that the structure of the corresponding temperature fields is found significantly different in relation with the Prandtl number values of the two fluids.

1. Introduction

The regular vortex street downstream of a bluff body at low Reynolds numbers ($30 < Re = U_\infty d/\nu_g < 80$) has always received much attention of researchers because of its practical importance as well as theoretical interest. Here U_∞ is the free stream velocity, d is the bluff body diameter and ν_g is the kinematic viscosity calculated at the free stream temperature. Although many aspects of the velocity field have been studied in detail, in both experimental and numerical approaches in isothermal flows, corresponding investigations of the temperature field in the forced and free convection regimes have not yet been achieved over this low Reynolds numbers range [1–3].

One of the main reason for this situation is linked to the experimental difficulty of carrying out accurate temperature measurements at low velocities in a wake of small dimensions. Furthermore, preliminary work carried out by the authors has shown that, over this Reynolds numbers range, the structure of the wake behind a heated bluff body was very sensitive to the heat input and that, even in absence of buoyancy effects, heat was never a passive contaminant. In fact due to the thermal dependence of the kinematic viscosity, it appears that heating the bluff body stabilizes the flow in a gas while it destabilizes the flow in a liquid [4–6]. This situation requires the use of an effective Reynolds number to characterize the flow regime downstream of a heated obstacle. This effective Reynolds number was associated to an effective temperature by Lecordier et al [4], Ezerski [5], and Paranthoën et al. [7].

This effective temperature (T_{eff}) was found to be for a heated cylinder in air:

$$T_{\text{eff}} = T_\infty + (0.24 \pm 0.02)\Delta T_w \tag{1}$$

where $\Delta T_w = T_w - T_\infty$. The value of this effective temperature is close to the hot recirculation zone temperature [8].

In this paper we present and discuss some recent results concerning the temperature field obtained suc-

* Corresponding author.

0017-9310/99/$ - see front matter
PII: S0017-9310(99)00010-1

Nomenclature

d	diameter of the ribbon [m]
g	gravitational acceleration [m s^{-2}]
Gr	Grashof number
I	current intensity
L	length of the ribbon [m]
Nu	Nusselt number
P	electric power [W]
Pe	Peclet number
Pr	Prandtl number
Re	Reynolds number
T	temperature [°C]
U	longitudinal velocity [m s^{-1}]
x	coordinate for horizontal axis [m]
y	coordinate for vertical axis [m]

Greek symbols

α	non-dimensional parameter
β	temperature coefficient for volume expansion [$°C^{-1}$]
κ	thermal diffusivity [m^2 s^{-1}]
ν	kinematic viscosity [m^2 s^{-1}]
ρ	density [kg m^{-3}]

Subscripts

c	critical
eff	refers to conditions at effective temperature
g	fluid
max	maximum
∞	free stream

cessively in water and air in the near wake of a heated flat ribbon at the same effective Reynolds number. The main motivation of this work is to investigate the influence of the Prandtl number on heat transport and mixing in a flow characterized by a laminar Bénard–Kármán vortex street.

2. Experimental set-up and procedures

The experiments, in air flows, were carried out in air in the potential core of a laminar plane jet which exits normally to an end plate (17×35 cm) from a slit 1.5 cm wide and 15 cm span centrally located in the plate. The vortex shedding bluff body was a nichrome ribbon (1×55 μm) mounted horizontally in the middle of the jet, close to the exit plane. Similar experiments have been made in a water channel by using a nichrome ribbon (3.2×75 μm). The critical Reynolds number Re_c, corresponding to the transition from a 2-D steady to a 2-D periodic wake, was found to be about 30 both in air and in water. The corresponding upstream velocities were 50 cm s^{-1} and 1 cm s^{-1}, respectively. These obstacles were heated by Joule effect and the heat input per unit length was about 20 W m^{-1}. In these conditions the ratio $\alpha = Gr/Re^2$ was about 10^{-4} in air and 0.05 in water corresponding to the forced convection regime in this cross flow geometry [9,10]. Here Gr is the Grashof number defined as $Gr = g\beta\Delta T_w d^3/\nu_g^2$, where g is the acceleration due to the gravity, β is the temperature coefficient for volume expansion and ΔT is the temperature difference between the obstacle and the upstream flow.

The upstream velocity was measured in air and in water using an LDA TSI system incorporating a 1.5 W Spectra-Physics laser system, an integrated optical transmission unit and a light collecting system for forward scattering mode. The optical measuring volume was $0.08 \times 0.08 \times 1$ mm^3.

Temperature measurements in the wake were made

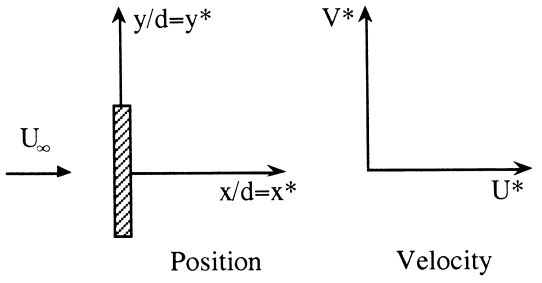

Fig. 1. Experimental set-up.

by using a cold wire in air and a thermocouple in water. This cold wire, Pt–Rh 10% Wollaston, was 0.4 mm in length and 0.7 μm in diameter and operated at constant current, $I = 0.1$ mA, using an inhouse circuit.

The thermocouples were built with 70 μm diameter Chromel and Alumel wires. The frequency responses of the cold wire and thermocouple were about 3500 Hz and 50 Hz, respectively and sufficient to measure the temperature fluctuations generated in the heated wake in air and in water. The vortex street frequencies were about 120 Hz and 1 Hz, respectively.

As shown in Fig. 1 the origin of the coordinate system was taken at the centre of the ribbon. The x axis was measured in the direction of the flow, the y axis was perpendicular to the flow. In our study all the lengths are non-dimensionalized by the width of the ribbon d. Re is the Reynolds number in isothermal conditions, i.e. calculated with the viscosity of the upstream flow.

3. Results

3.1. Effective Reynolds number

As already mentioned above, in the presence of a 2-D periodic wake $30 < Re < 80$, heating the flat ribbon is found to stabilize or to destabilize the flow in air and in water, respectively. This effect is related to both changes of the near wake dynamic viscosity and density with temperature and to the corresponding decrease or increase of the effective Reynolds number. In air, the effective Reynolds number (Re_{eff}) is lower than Re and in water Re_{eff} is larger than Re, which shows that over this Reynolds number range, the velocity field downstream of a heated cylinder depends on the level of heating. In the case of the cylinder, the use of an effective Reynolds number, associated to an effective temperature, $T_{\text{eff}} = T_\infty + (0.24 \pm 0.02)\Delta T_w$ where $\Delta T_w = T - T_\infty$, takes account of this effect. Here the ribbon temperature was not known and the effective Reynolds number (Re_{eff}) could not be deduced from the above relation. The effective Reynolds number was then deduced from the power density per unit length (P/L). It was assumed, as checked for the cylinder, that

$$\frac{Re - Re_{\text{eff}}}{Re - Re_c} = \frac{P/L}{P/L_{\text{crit}}} \tag{2}$$

where P/L_{crit} is the power per unit length needed to stabilize the wake.

In the case of water, the level of heating in our operating conditions was always very low in order to avoid buoyancy effects and the effective Reynolds number was approximately always equal to the usual Reynolds number, i.e. calculated in isothermal condition.

In order to compare the temperature field in the same flow regime, experiments were carried out in air and in water in the wake of heated ribbon for the same values of the effective Reynolds number: $Re_{\text{eff}} = Re_c + 3.3$ and $Re_{\text{eff}} = Re_c + 7.7$. These cases have been obtained for the following conditions:

$Re_{\text{eff}} = Re_c + 3.3$

($Re = Re_c + 3.3$, $P/L = 0$ W/m; $Re = Re_c + 7.8$, $P/L = 20$ W/m) in air

($Re = Re_c + 3.3$, $P/L = 0$ W/m; $Re = Re_c + 3.3$, $P/L = 20$ W/m) in water.

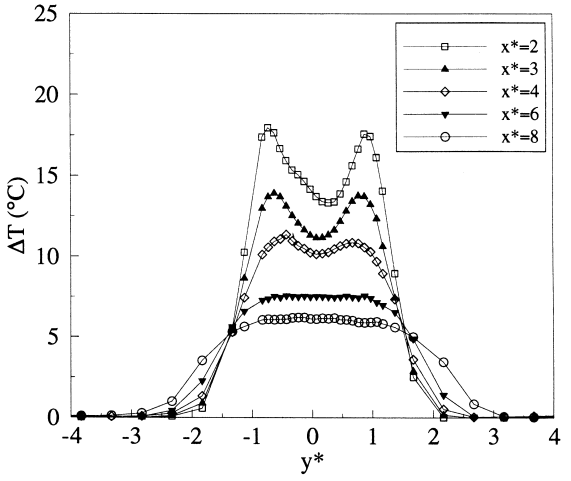

Fig. 2. Mean temperature profiles in air, $Re_{\text{eff}} = Re_c + 7.7$.

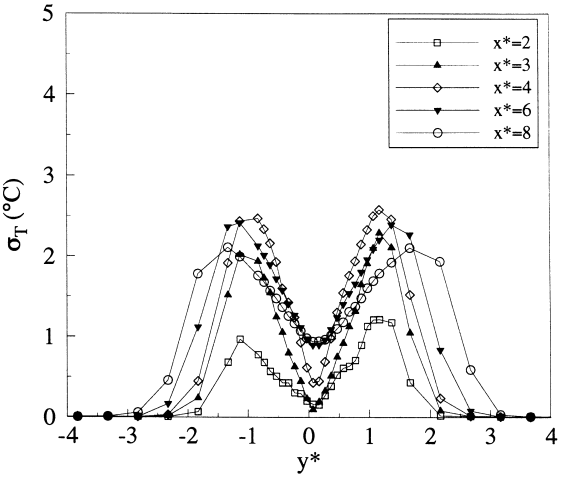

Fig. 3. R.m.s. temperature profiles in air, $Re_{\text{eff}} = Re_{\text{c}} + 7.7$.

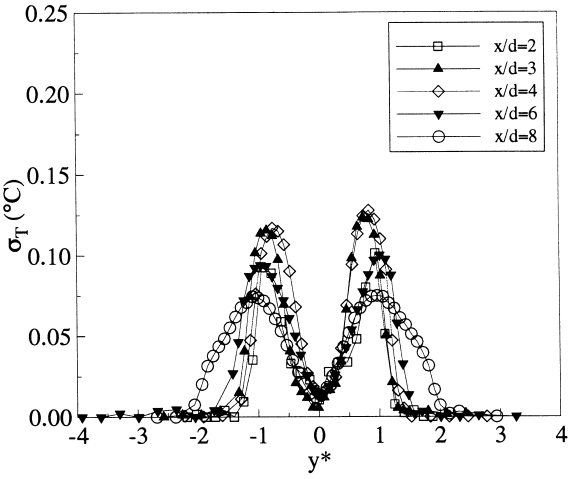

Fig. 5. R.m.s. temperature profiles in water, $Re_{\text{eff}} = Re_{\text{c}} + 7.7$.

$$Re_{\text{eff}} = Re_{\text{c}} + 7.7$$

($Re = R_{\text{c}} + 7.7$, $P/L = 0$ W/m; $Re = Re_{\text{c}} + 12.8$, $P/L = 20$ W/m) in air

($Re = Re_{\text{c}} + 7.7$, $P/L = 0$ W/m; $Re = Re_{\text{c}} + 7.7$, $P/L = 20$ W/m) in water.

3.2. Temperature profiles in air and in water

For an example, the mean temperature profiles measured in air in the heated wake of the ribbon at $Re_{\text{eff}} = Re_{\text{c}} + 7.7$ are presented in Fig. 2. The mean temperature profiles are nearly symmetrical about the wake axis and are only strongly double peaked at all the nearest sections, $x^* \leqslant 4$. The skewness of the mean temperature profile measured at $x^* = 2$ could be due to the perturbation of the probe. From $x^* = 6$ the mean temperature is almost constant when $-1 < y^* < 1$. The distributions of the corresponding values of r.m.s. temperature fluctuations are presented in Fig. 3 at various x^* positions. These distributions are also double peaked but with a centre line value increasing with x^* over the measured range.

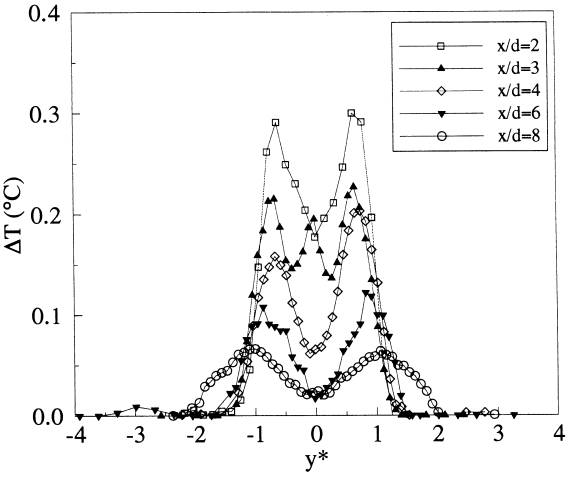

Fig. 4. Mean temperature profiles in water, $Re_{\text{eff}} = Re_{\text{c}} + 7.7$.

The mean temperature profiles measured in water in the heated wake of the ribbon at $Re_{\text{eff}} = Re_{\text{c}} + 7.7$ are presented in Fig. 4. These profiles are nearly symmetrical about the wake axis and are always strongly double peaked at all the sections. At $x^* = 3$, corresponding to about the end of the recirculation zone, the mean temperature profile has three peaks. The corresponding profiles of the r.m.s. of temperature fluctuations are presented in Fig. 5. These distributions are also strongly double peaked and nearly symmetrical about the wake axis. It is worth noting that, on the center line, the r.m.s. value of the temperature fluctuations is almost zero while the maximum value is located at approximately $y^* = 0.8$–1.

3.3. Comparisons of characteristics of temperature profiles in air and in water

Differences between experimental results, obtained in air and in water at the same effective Reynolds number ($Re_{\text{eff}} = Re_{\text{c}} + 7.7$), appear more clearly on the longitudinal evolution of the characteristics of the tempera-

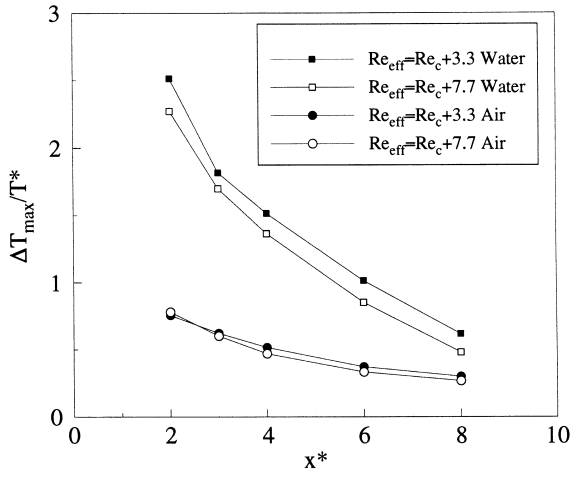

Fig. 6. Longitudinal evolution of the maximum mean temperature in air and in water; $Re_{\mathrm{eff}} = Re_{\mathrm{c}} + 3.3$ and $Re_{\mathrm{c}} + 7.7$.

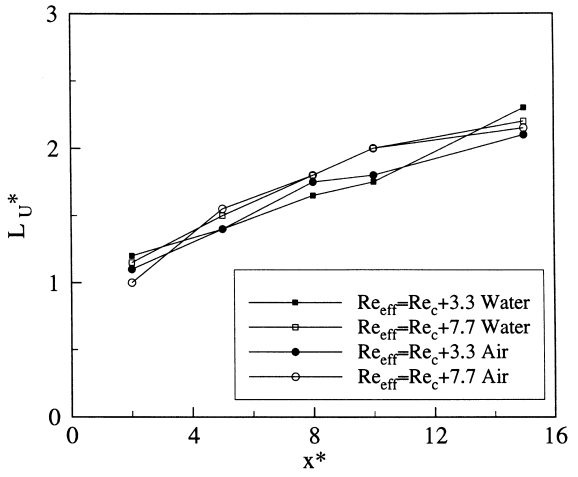

Fig. 8. Longitudinal evolution of the width of mean velocity profiles in air and in water; $Re_{\mathrm{eff}} = Re_{\mathrm{c}} + 3.3$ and $Re_{\mathrm{c}} + 7.7$.

ture fields. In these comparisons measurements obtained at $Re_{\mathrm{eff}} = Re_{\mathrm{c}} + 3.3$ have also been included.

The global characteristics of the temperature field including the maximum mean temperature $\Delta T_{\max}$, the width of the mean temperature profile L_T^* and the maximum value of the intensity of temperature fluctuations $\sigma T_{\max}/\Delta T_{\max}$ are presented in Figs. 6–9. In Fig. 6 the longitudinal evolution of the normalized maximum mean temperature $\Delta T_{\max}/T^*$ is presented by using the temperature scale $T^* = P/\rho C_{\mathrm{p}} U_\infty dL$. It appears that the normalized maximum mean temperature is about three times higher in water than in air. The width L_T^* of the mean temperature profiles, defined as the location where $\Delta T(L_T) = \Delta T_{\max}/2$ are shown in Fig. 7. In the near wake L_T^* is always larger in air than in water, while after $x^* = 8$ the difference between the widths of the mean temperature profiles is reduced. For comparison the longitudinal evolution of the width L_{u}^* of the velocity profiles, defined by $U(L_{\mathrm{u}}) = (U_{\max} - U_{\mathrm{cl}})/2$ is also presented Fig. 8. The level of the intensity of temperature fluctuations $\sigma T_{\max}/\Delta T_{\max}$ obtained in these two cases are plotted in Fig. 9. As shown in this figure, over the studied range the intensity of temperature fluctuations in the heated vortex street is always increasing and is found to be about three to four times higher in water than in air.

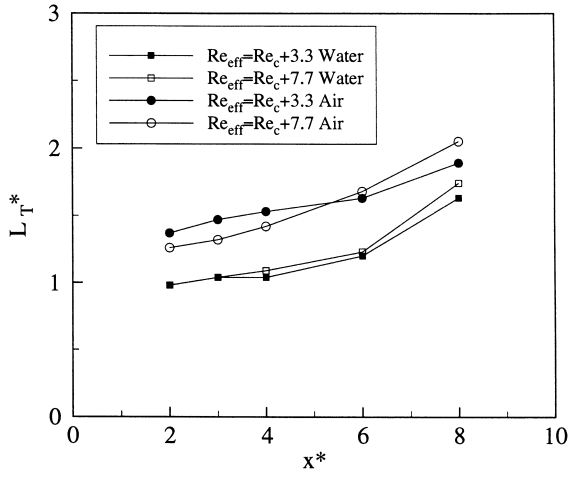

Fig. 7. Longitudinal evolution of the width of mean temperature profiles in air and in water; $Re_{\mathrm{eff}} = Re_{\mathrm{c}} + 3.3$ and $Re_{\mathrm{c}} + 7.7$.

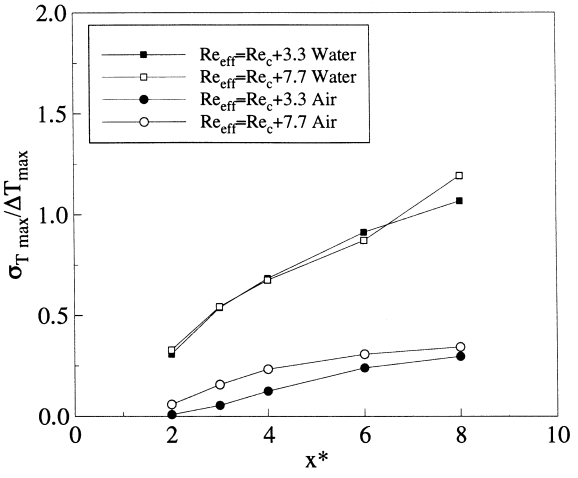

Fig. 9. Longitudinal evolution of the maximum intensity of temperature fluctuations in air and in water; $Re_{\mathrm{eff}} = Re_{\mathrm{c}} + 3.3$ and $Re_{\mathrm{c}} + 7.7$.

5. Discussion

As presented in previous results [11,12], in air and in water the velocity fields measured at the same effective Reynolds number are found similar in the two fluids. It appears that the corresponding temperature fields are significantly different. For example, the maximum mean temperature is found much higher than the centreline mean temperature in water and close to the centreline mean temperature in air. In parallel, the level of the intensity of temperature fluctuations in air is much lower than that obtained in the water flow.

These differences can be explained by the larger value of the Prandtl number $Pr = \nu_g/\kappa_g$ in water ($Pr \approx 7$) than in air ($Pr \approx 0.7$), which shows that in experiments being performed at the same Reynolds number, the Peclet numbers $Pe = U_\infty d/\kappa_g$ are significantly different in air ($Pe \approx 26$) and in water ($Pe \approx 260$). In the case of the water flow, due to the relative lower value of the thermal diffusivity κ_g in comparison with the kinematic viscosity, the heat is initially more concentrated in the initial shear layers and then within the laminar vortices of the wake. This explains the higher value of the mean peak temperature and the lower values of the width of the temperature field. Furthermore, this lower influence of thermal diffusion in water increases the intermittent character of the temperature signal measured in the wake and the stronger increase of the maximum intensity of temperature fluctuations with the distance. This result is similar to results obtained downstream an heated line source located in turbulent flow. In this latter case the maximum intensity of temperature fluctuations is dependent on the ratio between the instantaneous plume width and the Lagrangian length scale of the flow [13,14]. In our case the velocity fields which carry on the heat are similar while the instantaneous temperature fields have to be different in air and in water. The instantaneous width of the temperature profile is always much smaller in water than in air due to the respective values of Prandtl numbers. It results that in similar flow conditions the level of temperature fluctuations is always higher in water than in air.

5. Conclusion

Experimental study of temperature fields measured in air and in water in the 2-D periodic near wake of a heated ribbon has been carried out in absence of buoyancy effects. The opposite thermal dependence of the kinematic viscosity in a gas and in a liquid and the resulting stabilizing and destabilizing character leads to use the effective Reynolds number approach. When the experiments are carried out in air and in water at the same effective Reynolds number, i.e. in similar flow conditions in the wake, it appears that the temperature fields in these two fluids are strongly different. The shape of the temperature profiles is not the same. The peak value of the mean temperature and the maximum intensity of temperature fluctuations are much higher in water than in air. Conversely the widths of the temperature profiles are much narrow in water than in air. These results can be related to the influence of the Prandtl number of the two fluids on the diffusion of heat in the initial shear layers and then within the vortices in the near wake of the heated ribbon.

References

[1] C.H.K. Williamson, Oblique and parallel modes of vortex shedding in the wake of a circular cylinder at low Reynolds numbers, J. Fluid Mech. 206 (1989) 579–627.
[2] S. Goujon-Durand, P. Jennfer, J.E. Wesfreid, Downstream evolution of the Bénard–Kármán instability, Phys. Rev. E 50 (1) (1994) 308–313.
[3] X. Yang, A. Zebib, Absolute and convective instability of a cylinder wake, Phys. Fluids A 1 (4) (1989) 689–696.
[4] J.C. Lecordier, L. Hamma, P. Paranthoën, The control of vortex shedding behind heated circular cylinders at low Reynolds numbers, Exp. in Fluids 10 (1991) 224–229.
[5] A.B. Ezerski, Detached flow around a heated cylinder at small Mach number, Prikladnaya Mekhanika i Tekhn. Fizika 5 (1990) 56–62.
[6] L. Socolescu, I. Mutabazi, O. Daube, S. Huberson, Etude de l'instabilité du sillage 2D derrière un cylindre faiblement chauffé, C.R. Acad. Sciences Paris, 1996. t 322, Serie IIb, pp. 203–208.
[7] P. Paranthoën, L.W.B. Browne, S. Le Masson, J.C. Lecordier, Control of vortex shedding by thermal effect at low Reynolds number, Int Rept. MT1, Rouen University, 1995.
[8] F. Dumouchel, J.C. Lecordier, P. Paranthoen, The effective Reynolds number of a heated cylinder, Int. J. Heat Mass Transfer 41 (1998) 1787–1794.
[9] V.T. Morgan, The overall convective heat transfer from smooth circular cylinders, Adv. Heat Transfer 11 (1975) 199–263.
[10] R.M. Fand, K.K. Keswani, Combined natural and forced convection heat transfer from horizontal cylinders to water, Int. J. Heat Mass Transfer 16 (1973) 1175–1191.
[11] J.C. Lecordier, L.W.B. Browne, S. Le Masson, F. Dumouchel, P. Paranthoën, Control of vortex shedding by thermal effect at low Reynolds numbers (in preparation).
[12] F. Dumouchel, Etude expérimentale des champs dynamiques et thermiques de l'écoulement de Bénard–Kármán en aval d'un obstacle chauffé dans l'air et dans l'eau, Thèse Sciences Physiques, Université de Rouen, 1997.
[13] J.L. Lumley, I. van Cruyningen, Limitations of second order modeling of passive scalar diffusion, in: Frontiers in Fluid Mechanics, Springer Verlag, Berlin, Heidelberg, 1985, pp. 199–217.
[14] P. Paranthoën, A. Fouari, A. Dupont, J.C. Lecordier, Dispersion measurements in turbulent flows, Int. J. Heat Mass Transfer 31 (1988) 153–165.